Electronic Supplementary Information

Optimizing the Charge Transfer Process by Design of Co_3O_4@PPy@MnO_2 Ternary Core-Shell Composites

Bin Wang, Xinyi He, Hongpeng Li, Qi Liu, Jun Wang, Lei Yu, Huijun Yan, Zhanshuang Li, Peng Wang*

Experimental Sections

Synthesis of Co_3O_4 nanowires.

Co_3O_4 nanowires were grown on Cu substrate by a modified hydrothermal process as reported previously. Cu substrate was washed with suds, water and ethanol. To control the growth of only one side, we sealed the other side with imide tape. Then the prepared Cu substrate was put into a solution of 0.15 M $CoCl_2 \cdot 6H_2O$ and 6 g NH_2CO and reacted at 60 ℃ for 8 h. Then the Cu substrate covered with products was washed successively with deionized water and ethanol, and then dried. Finally, the as-prepared samples were calcined at 250 ℃ for 2 h in Ar ambiance.

Coating PPy (PANI) onto Co_3O_4 nanowires.

PPy (PANI) was grown onto the Co_3O_4 nanowires by a simple monomer polymerization process. Ethanol solution (with 0.008 M p-TSA and 0.0048 M pyrrole (aniline) monomer) and an aqueous solution (with 0.00263 M ammonium persulfate0 were prepared. The Cu substrate (coated Co_3O_4 nanowires, with the other side sealed with imide tape) was tiled on the surface plate. The ethanol solution was slowly

dropped onto the surface to ensure the surface was covered totally. Then the aqueous solution was dropped to cover the surface. The sample reacted in the dark for 7 h. Finally Co_3O_4@PPy (Co_3O_4@PANI) was washed with water and ethanol, and dried under room temperature.

The growth of MnO_2.

Co_3O_4@PPy (the side without Co_3O_4@PPy was sealed with imide tape) was put into manganese acetate solution (6 mM) for 2min, then taken out and put into $KMnO_4$ solution (4 mM) for 1 min and washed with water. Repetition of the above steps can increase the mass of MnO_2. Finally, Co_3O_4@PPy@MnO_2 was dried at room temperature. The process of growing MnO_2 onto Co_3O_4@PANI was carried out in the same way.

The growth of NiOOH.

The growth of NiOOH was carried out by a chemical bath deposition (CBD) method. Solution for CBD was prepared by adding 10 mL of aqueous ammonia (25~28%) to the mixture of 40 mL of 1 M Ni sulfate and 30 mL of 0.25 M potassium. The pretreated Co_3O_4@PPy (the side without Co_3O_4@PPy was sealed with imide tape) was vertically placed in solution for 5 min at room temperature, then washed with deionized water and dried. The growth of NiOOH on Co_3O_4@PANI was carried out in the same way.

Characterization Methods

The crystallographic structures of the materials were characterized by a powder X-ray diffraction system (XRD, TTR-III) equipped with Cu Kα radiation (λ = 0.15406 nm). The X-ray photoelectron spectroscopy (XPS) measurements were characterized by a PHI 5700 ESCA spectrometer with a monochromated Al Kα radiation (hv=1486.6 eV). All XPS spectra were corrected using the C 1s line at 284.6 eV. Fourier-transform infrared (FT-IR) spectrum was recorded with an AVATAR 360 FT-IR spectrophotometer using a standard KBr pellet technique. The microstructure of the samples was investigated by scanning electron microscopy (SEM, Hitachi SU8010) and transmission electron microscopy (TEM, PHILIPS CM 200 FEG, 160 kV).

Electrochemical measurement was carried out on a CHI 660D electrochemistry workstation. Cyclic voltammetry (CV) measurements, galvanostatic charge/discharge (CD) and electrochemical impedance spectroscopy (EIS) were studied on a three-electrode system, and the electrolyte was 1 M KOH aqueous solution. All tests were carried out at room temperature. The mass of the electrodes was calculated based on the whole area of 10 cm^2.

The specific capacitance (C_s, Eq.1) and the specific area capacitance (C_a, Eq.2) of the composites were calculated as follows:

$$C_s = \frac{I * t}{V} \quad (1)$$

$$C_a = C_s * m \quad (2)$$

where I, t, V and m are the constant current density (A/g), the discharge time (s), the total potential deviation (V) and the mass loading of the active materials, respectively.

Table S1 Compared R_{ct} for different core-shell structured composites.

Core/Shell Structure Applied in Supercapacitors				
Materials	**Electrolyte**	***R_{ct}* Ω**	***C_{sp} F/g***	**Ref**
Co_3O_4@MnO_2	KOH (1M)	**60.9**	**265 (0.5 A/g)**	**This Work**
Co_3O_4@PPy		**12.87**	**360 (0.5 A/g)**	
Co_3O_4@PPy@MnO_2		**0.94**	**782 (0.5 A/g)**	
VACNF@MnO_2	Na_2SO_4 (0.1M)	154.6	318 (2.3 A/g)	21
MWCNT@MnO_2	Na_2SO_4 (0.5M)	60	380 (5 A/g)	30
Co_3O_4@MnO_2	LiOH (1M)	≈40	480 (2.67 A/g)	8
MnO_2/Mn/MnO_2	Na_2SO_4 (1M)	≈36	955 (1.5 A/g)	20
MnO_2-NiO	LiOH (1.5M)	18.7	0.4 (F/cm^2)	16
Zn_2SnO_4/MnO_2	Na_2SO_4 (1M)	4.9	642.4 (1 A/g)	9
Carbon nanofiber/MnO_2	Na_2SO_4 (1M)	4	311 (2 mV/s)	42
ZnO@MnO_2	Na_2SO_4 (0.5M)	2.74	1261 (1 mA/cm^2)	43
MnO_2/CNTs-CNFs	Na_2SO_4 (0.1M)	2.6	357 (1 A/g)	33
NiO/CAMB	KOH (6M)	3.52	356 (1 A/g)	32
Ni–Co oxides NWs@TiO2	NaOH (1M)	2.4	2353 (2.5 A/g)	17
CoO@PPy	NaOH (3M)	0.5	2220 (1 mA/cm^2)	29
Co_3O_4@NiO	KOH (2M)	≈0.3	853 (2 A/g)	22
Ni-Doped $Co(OH)_2$/Ti	KOH (1M)	53.6	894 (1 A/g)	34
Ni-Doped $Co(OH)_2$/ITO		12.8	2052 (1 A/g)	
NiO/Ti	KOH (1M)	125.3	416 (1 A/g)	35
NiO/ITO		12.5	1025 (1 A/g)	
MnO_2/Ti	Na_2SO_4 (0.5M)	166.6	439 (1 A/g)	10
MnO_2/ITO		89.6	821 (1 A/g)	
CoO@TiO_2	KOH (2M)	≈4.5	187 (10 mA/cm^2)	36
CoOΘTiO_2		≈0.6	633 (10 mA/cm^2)	

Core/Shell Structure Applied in Lithium Ion Battery				
Materials	**Electrolyte**	***R_{ct}* Ω**	***C mAh/g***	**Ref**
V_2O_5/PEDOT		158	175 (50mA/g)	18
V_2O_5/PEDOT&MnO_2 NWs		74	179 (50mA/g)	
MnO_2/C		128.5	741 (0.1 A/g)	31
TiO_2-C		82.1	576 (167.5mA/g)	19
TiO_2-C/MnO_2		49.2	865 (167.5mA/g)	

Figure S1. SEM images of core-shell composites.

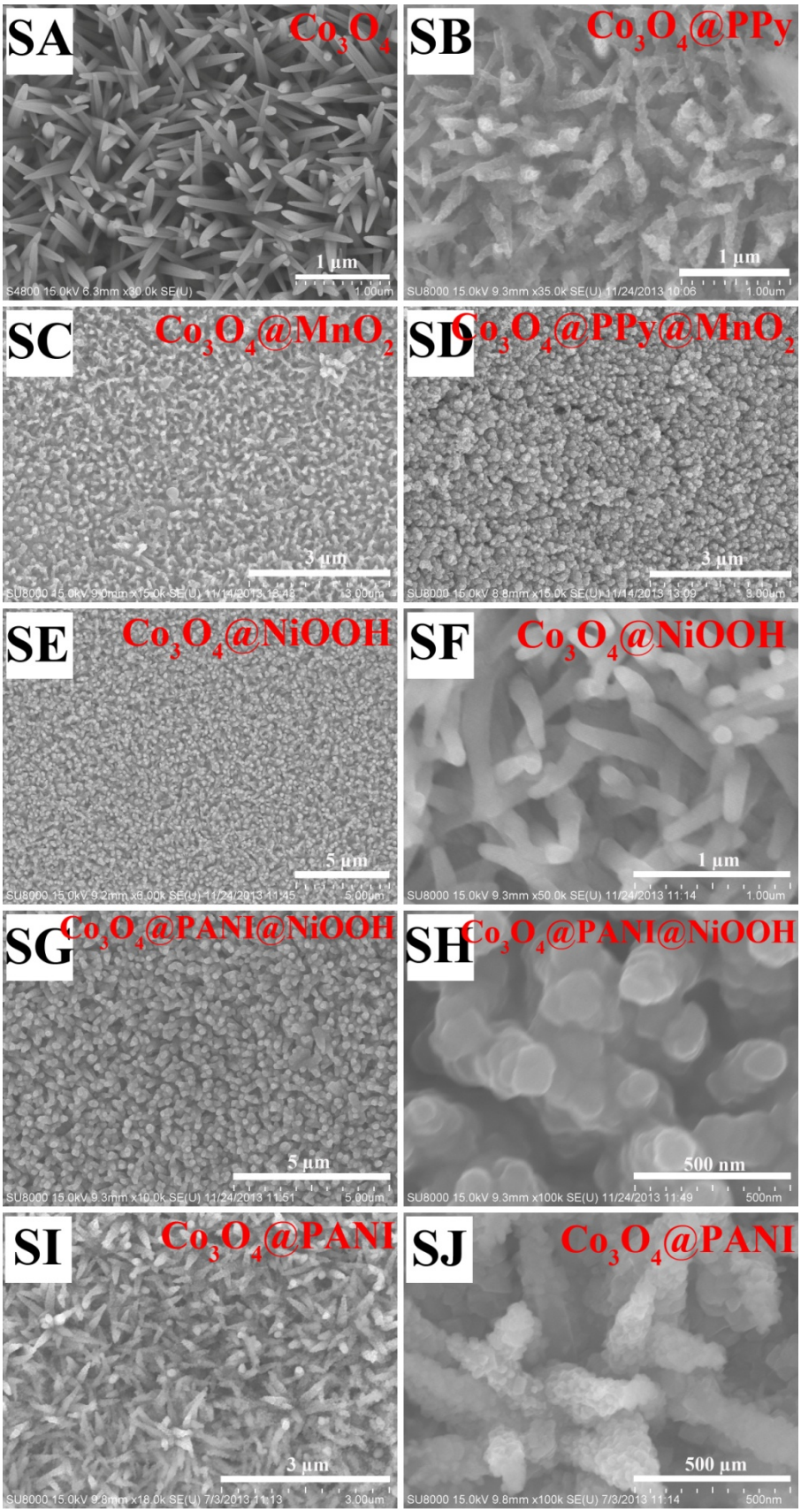

Figure S2. The resulting TEM images of core-shell composites.

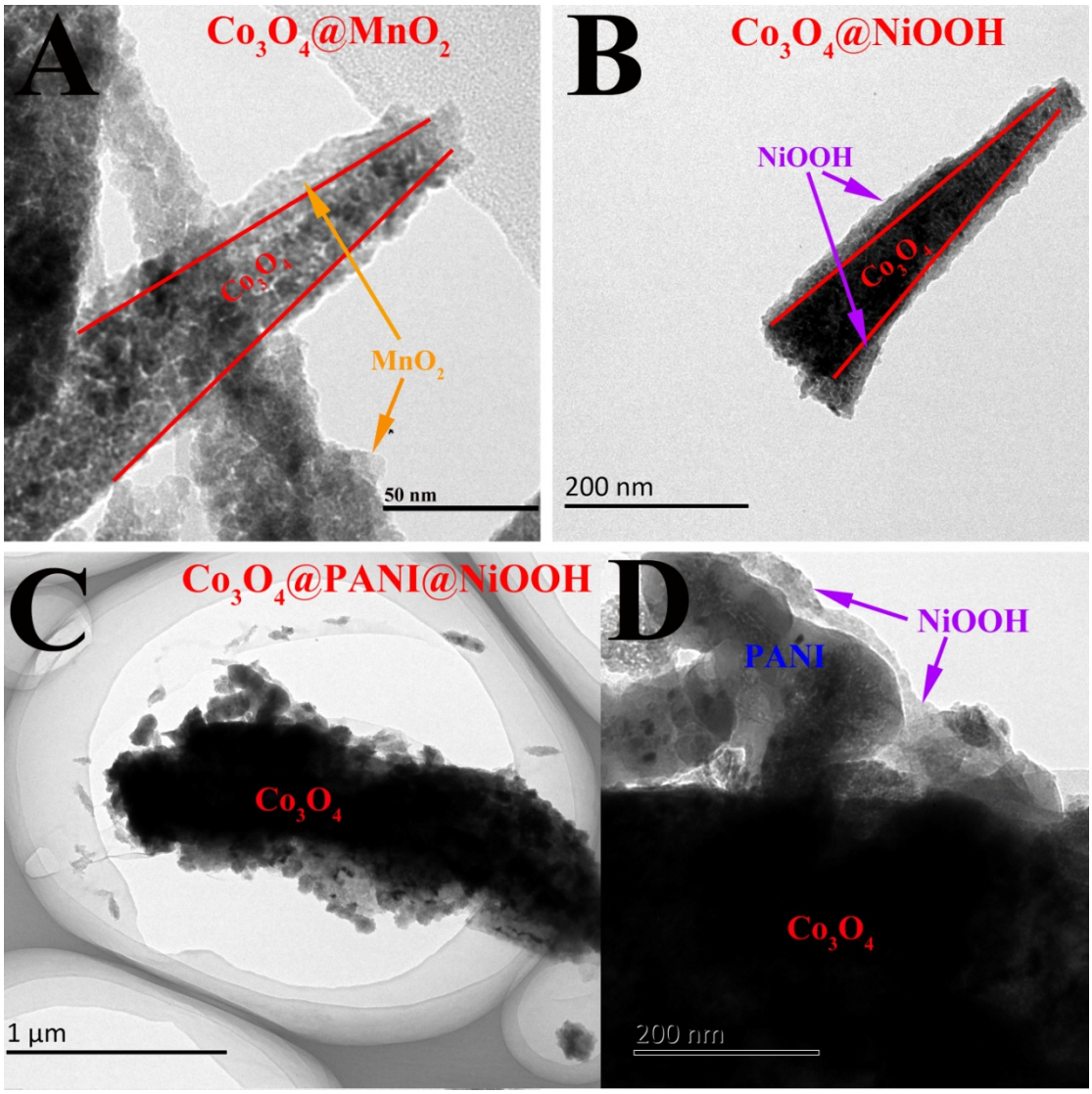
A
Co3O4@MnO2
Co3O4
MnO2
50 nm
B
Co3O4@NiOOH
NiOOH
Co3O4
200 nm
C
Co3O4@PANI@NiOOH
Co3O4
1 µm
D
NiOOH
PANI
Co3O4
200 nm

Figure S3. EDS mapping results from Co_3O_4@MnO_2 binary core-shell hierarchical structure.

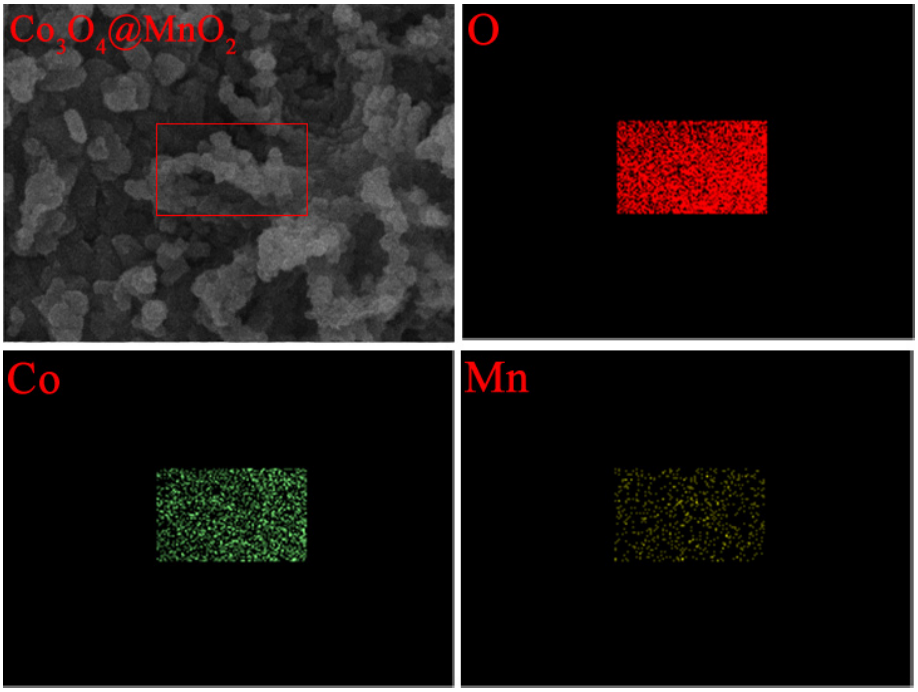

Figure S4. EDS mapping results from Co_3O_4@PPy@MnO_2 ternary core-shell hierarchical structure.

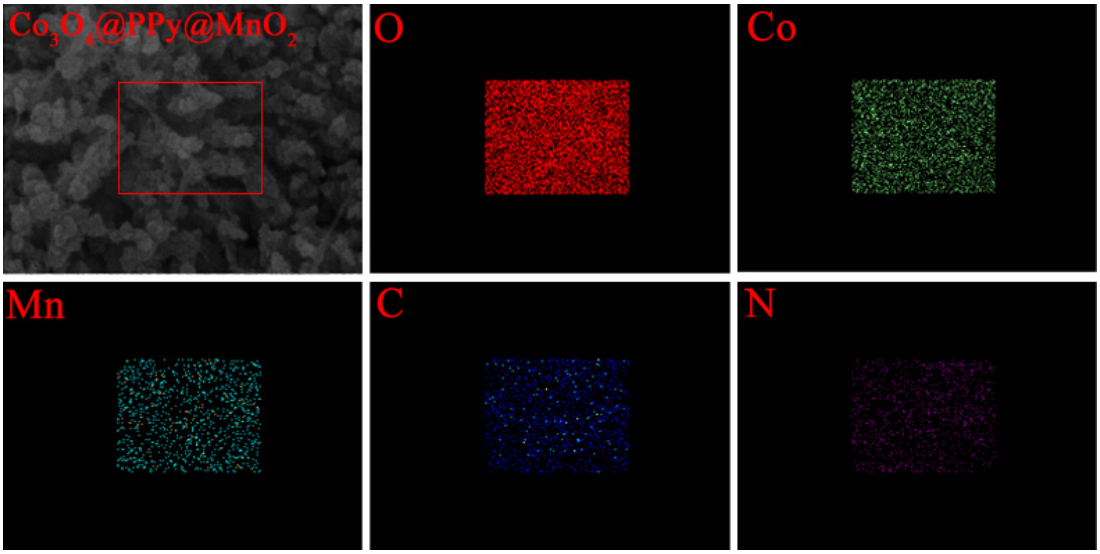

Figure S5. CV and CD curves of pure Co_3O_4, Co_3O_4@PPy and Co_3O_4@MnO_2.

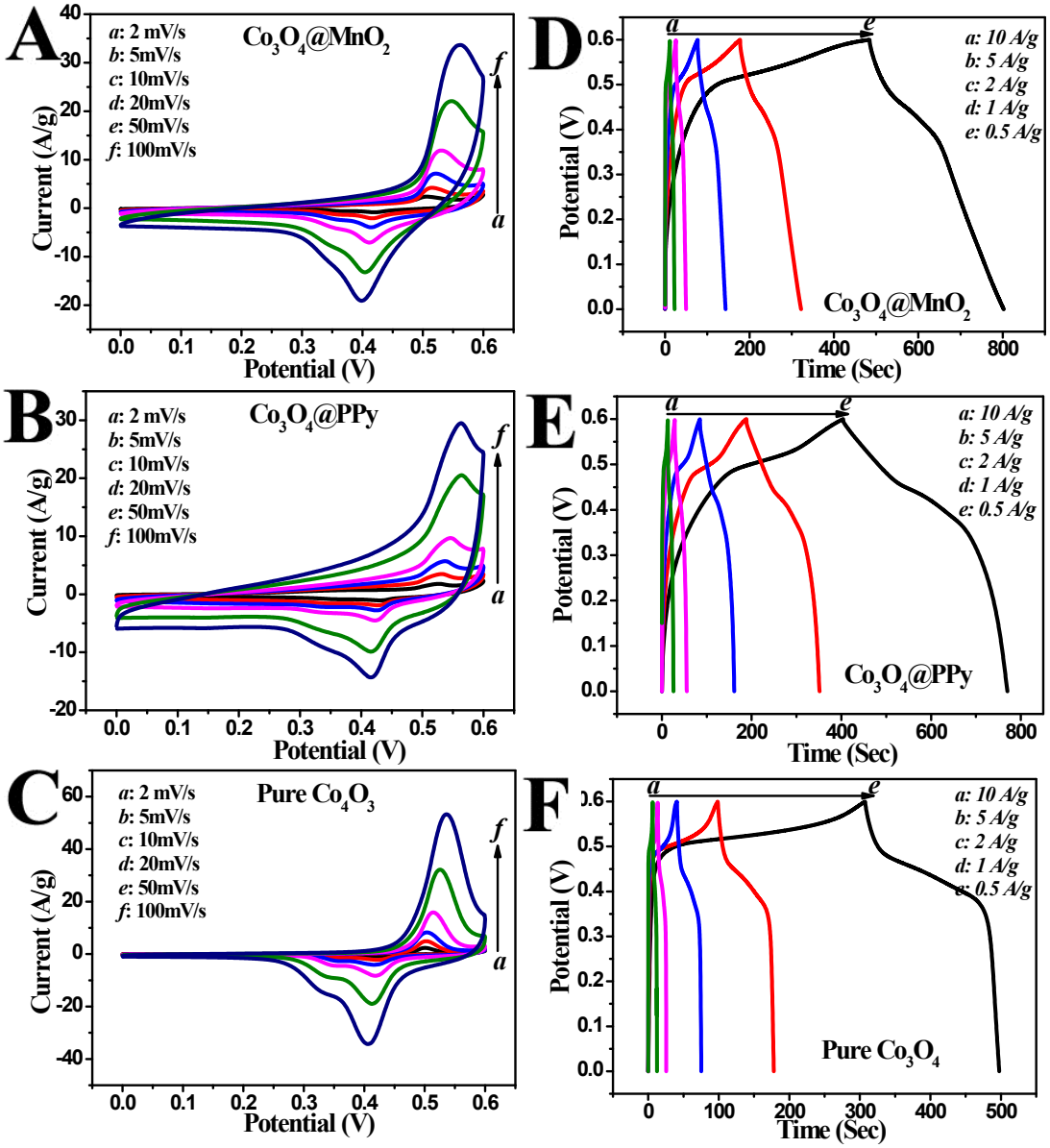

Figure S6. Specific area capacitances of the composites.

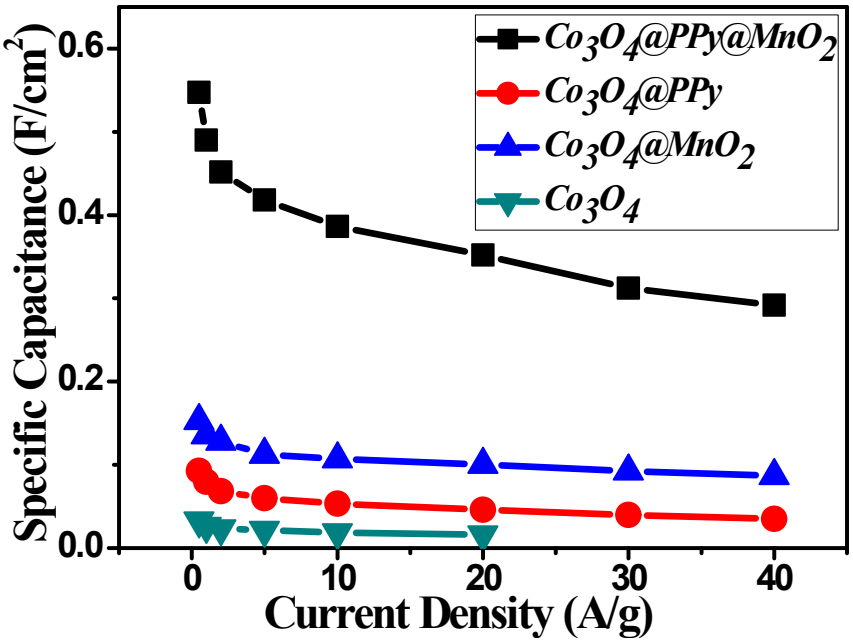

Table S7. Detailed EIS information of the composites.

	R_s	R_{ct}
Co_3O_4@PPy	0.8634	**12.87**
Co_3O_4@MnO_2	0.96	**60.9**
Co_3O_4@PANI	0.62	**13.1**
Co_3O_4@NiO	0.9243	**20.63**
Co_3O_4@PPy@MnO_2-4	0.957	**0.9408**
Co_3O_4@PANI@MnO_2-4	0.45	**1.764**
Co_3O_4@PPy@NiOOH	0.87	**1.361**
Co_3O_4@PANI@NiOOH	0.8443	**0.6025**
Co_3O_4@PPy@MnO_2-5	0.88	**1.915**
Co_3O_4@PPy@MnO_2-6	1.066	**2.006**
Co_3O_4@PPy@MnO_2-8	1.106	**8.897**
Co_3O_4@PPy@MnO_2-10	1	**11.55**
Co_3O_4@PANI@MnO_2-2	0.46	**1.153**
Co_3O_4@PANI@MnO_2-6	0.59	**4.061**

Figure S8 Comparison of CV, CF and EIS for Co_3O_4@PPy@NiOOH, Co_3O_4@NiOOH and Co_3O_4@PPy.

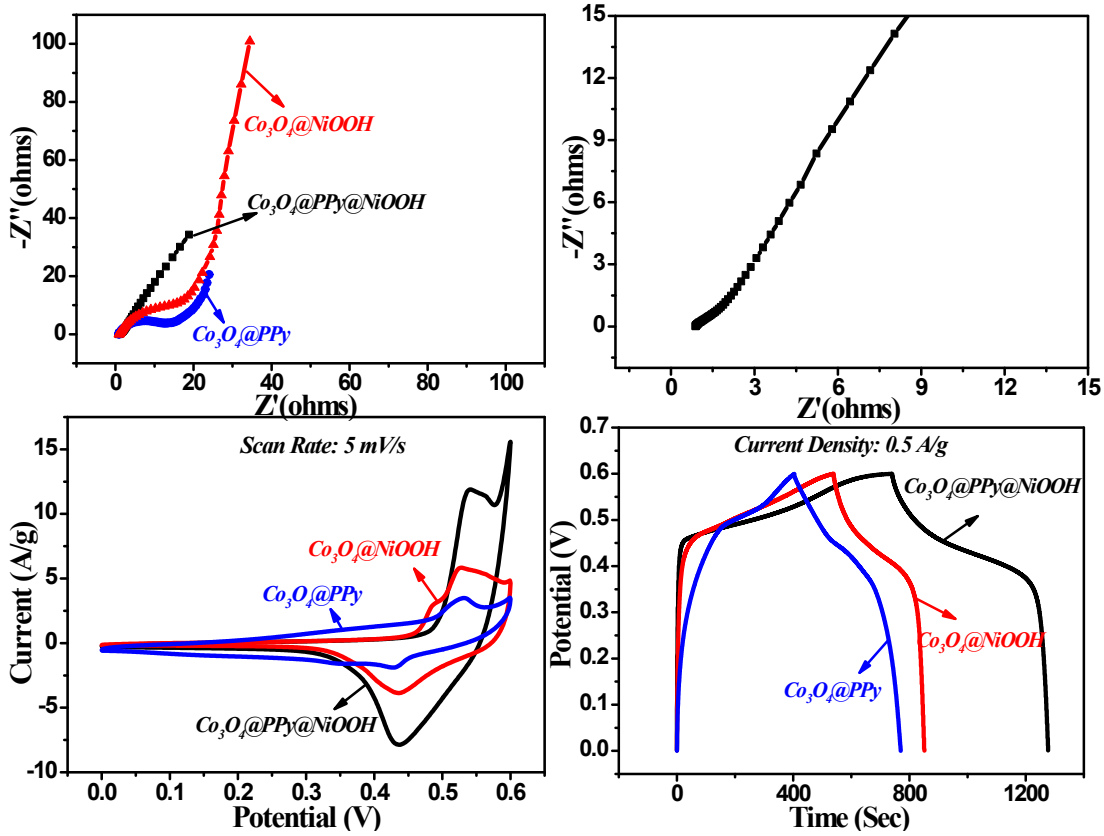

Figure S9 Compared CV, CF and EIS of Co_3O_4@PANI@MnO_2, Co_3O_4@MnO_2 and Co_3O_4@PANI.